bicyclo[3.3.1]nonan-2-one (26). Triethylamine (17 μL, 0.12 mmol) was added to a magnetically stirred solution of dibutylboron triflate (31 μL, 0.12 mmol) in 2 mL of dry Et_2O. The solution was cooled to −78 °C, and a solution of **25** (20 mg, 0.11 mmol) in 200 mL of Et_2O was added. The formation of a white precipitate was noted upon completion of the addition. The resulting solution was stirred for 30 min, and then propionaldehyde (10 μL, 0.134 mmol) was added. The reaction was stirred for 30 min at −78 °C, warmed to room temperature and stirred for 30 min, poured into water (5 mL), and extracted with Et_2O (3 × 10 mL). The organic extracts were concentrated, and the residue was dissolved in 1 mL of MeOH. This solution was then treated with 200 μL of 30% aqueous H_2O_2 solution and stirred for 15 min at room temperature. The reaction was poured into water (5 mL) and extracted with Et_2O (3 × 10 mL). The organic layers were combined, dried (K_2CO_3), and concentrated. Purification by silica gel gradient column chromatography (hexane/EtOAc: 7/1, 4/1, 2/1, 1 column volume each) afforded 19 mg (66%) of **26** as a clear colorless oil. Data for **26**: ^1H NMR (200 MHz, $CDCl_3$) 5.82 (m, 1 H), 5.01 (m, 2 H), 4.21 (m, 1 H), 3.59 (m, 1 H), 2.88 (m, 1 H), 2.54 (s, br, 1 H), 2.25–1.21 (m, 11 H), 0.97 (s, 3 H), 0.87 (t, 3 H).

Acknowledgment. We gratefully acknowledge financial support for this project from the National Science Foundation (Grant Nos. NSF CHE 8515371 and 881847). S.E.D. acknowledges support from the National Science Foundation (Presidential Young Investigator Award, 1985–1990), the Alfred P. Sloan Foundation (1985–1989), and the Alexander von Humboldt Foundation or a Senior Scientist Award (1990). B.R.H. thanks the University of Illinois for a graduate fellowship (1984–1988).

Syntheses and Properties of Soluble Carceplexes[1,2]

John C. Sherman, Carolyn B. Knobler, and Donald J. Cram*

Contribution from the Department of Chemistry and Biochemistry, University of California at Los Angeles, Los Angeles, California 90024. *Received August 31, 1990*

Abstract: The syntheses and characterizations of three soluble carceplexes (**1**·G, where G is guest) are reported. Carcerands are noncollapsible molecular cells whose interiors are large enough to contain molecules or ions (guests) and whose closed surfaces contain pores too small for guest molecules to enter or depart from their interiors without making or breaking covalent bonds. A carceplex is composed of a carcerand containing at least one guest (prisoner) molecule in its interior. The carceplexes reported here differ only in their guest structures. Their shell is shaped like a U.S. football, to which are attached around each of their small ends four phenylethyl groups for solubilization. The carceplexes were made by shell-closing two identical bowl-shaped cavitands (**2**), each containing on their rims four phenolic hydroxyls. The reaction was $2(ArOH)_4 + 4CH_2BrCl + 4Cs_2CO_3 \rightarrow (ArOCH_2OAr)_4 + 4CsBr + 4CsCl + 4CO_2 + 4H_2O$, in which eight covalent bonds were formed. In each synthesis, one molecule of solvent was encapsulated in remarkably good yield, leading to **1**·$(CH_3)_2SO$ (61%), **1**·$(CH_3)_2NCOCH_3$ (54%), and **1**·$(CH_3)_2NCHO$ (49%). The reaction, when run in $CH_2(CH_2CH_2)_2NCHO$, a solvent too large to be encapsulated, gave only polymers, indicating that the shell closures must be templated by the molecule that is ultimately incarcerated. A shell closure run in equimolar $(CH_3)_2NCOCH_3$–$(CH_3)_2NCHO$ gave a 27% yield of a mixture of **1**·$(CH_3)_2NCOCH_3$ and **1**·$(CH_3)_2NCHO$ (ratio 5.3), the mixture being separated chromatographically. Each carceplex's desorption chemical ionization mass spectra (DCI MS) gave substantial $M^+ + 1$ peaks. The ^1H and ^{13}C NMR spectra of each carceplex were taken, and all protons were assigned. All guest protons were moved upfield from their normal resonances by 1–4 ppm. Incarcerated $(CH_3)_2NCHO$ rotates about the host's short equatorial and long polar axes rapidly on the ^1H NMR time scale, even at −38 °C ($CDCl_3$); rotation of incarcerated $(CH_3)_2NCOCH_3$ about the host's long axis is fast, but about the short axes is slow, even at 175 °C ($C_6D_5NO_2$); incarcerated $(CH_3)_2SO$ rotations about all axes are fast above 2 °C, but slow about the short axes below 2 °C ($CDCl_3$). The rates of rotation about the C–N bond of amide guests vary with phase changes ($C_6D_5NO_2$ solvent when needed) as follows: for $(CH_3)_2NCHO$, vacuum > *interior phase* > solution; for $(CH_3)_2NCOCH_3$, vacuum > solution > *interior phase*. The crystal structures of **1**·$(CH_3)_2NCOCH_3$ and **5** correspond to those expected from scale molecular model examination.

Carcerands are closed-surface, globe-shaped compounds with enforced hollow interiors large enough to incarcerate simple organic compounds, inorganic ions, or both. Carceplexes are carcerands whose interiors are occupied by prisoner molecules or ions that cannot escape their molecular cells without breaking covalent bonds between the atoms that block their escape. We reported the syntheses of the first carceplexes[3a,b] (**Ia**) as inseparable, insoluble mixtures whose components possessed the same shell, but differed as to their prisoner molecules and ions (guests or G). The guests were identified by FAB MS, elemental analyses, and ^1H NMR spectra to be $(CH_3)_2NCHO$, $(CH_2)_4O$, Cs^+, argon, and $ClCF_2CF_2Cl$,[3] each of which was present in the medium used for shell closure of the two cavitands in the synthesis. The insolubility of these carceplexes prevented their isolation, characterization, and study as single chemical entities.

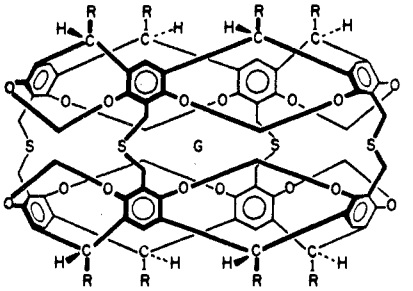

Ia, R = CH_3; **Ib**, R = $CH_2CH_2C_6H_5$; **Ic**, R = $(CH_2)_4CH_3$

The present and a companion study[4] were undertaken to overcome this limitation by appending eight long and conformationally mobile hydrocarbon groups to the carceplexes arranged in two groups of four around the arctic and antarctic circles of

(1) (a) We warmly thank the National Science Foundation for Grant CHE 88 02800, which supported this work. (b) Host–Guest Complexation. 56.

(2) Some of these results were previously communicated. Sherman, J. C.; Cram, D. J. *J. Am. Chem. Soc.* **1989**, *111*, 4527–4528.

(3) (a) Cram, D. J.; Karbach, S.; Kim, Y. H.; Baczynskyj, L.; Kalleymeyn, G. W. *J. Am. Chem. Soc.* **1985**, *107*, 2575–2576; (b) Cram, D. J.; Karbach, S.; Kim, Y. H.; Baczynskyj, L.; Marti, K.; Sampson, R. M.; Kalleymeyn, G. W. *Ibid.* **1988**, *110*, 2554–2560.

(4) Bryant, J. A.; Blanda, M. T.; Vincenti, M.; Cram, D. J. *J. Chem. Soc. Chem. Commun.* **1990**, 1403–1405.

0002-7863/91/1513-2194$02.50/0

Chart I

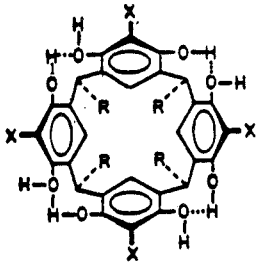

3, R = $CH_2CH_2C_6H_5$, X = H
4, R = $CH_2CH_2C_6H_5$, X = Br

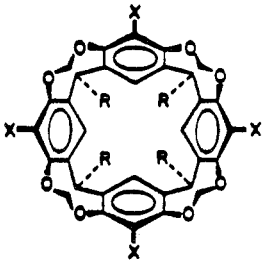

5, R = $CH_2CH_2C_6H_5$, X = Br
2, R = $CH_2CH_2C_6H_5$, X = OH
6, R = CH_3, X = Br

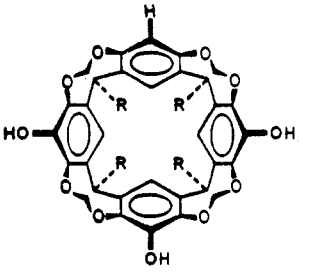

7, R = $CH_2CH_2C_6H_5$

the globes drawn in Ib, Ic, and **1**·G. Here, we report the syntheses, purifications, and physical and chemical properties of **1**·$(CH_3)_2SO$, **1**·$(CH_3)_2NCOCH_3$, and **1**·$(CH_3)_2NCHO$. In particular, we were interested in a complete characterization of the movements of the prisoner molecules (G) with respect to their cells (H) and in obtaining a crystal structure of a carceplex.

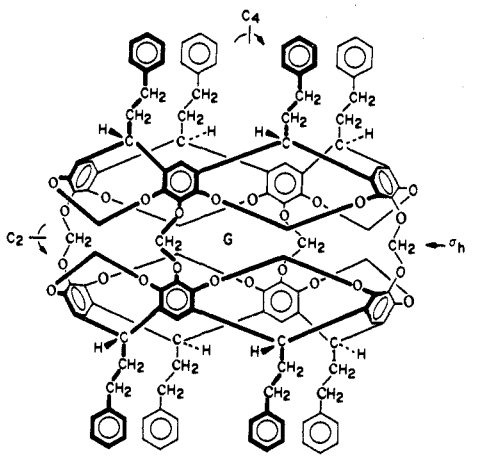

1·(CH3)2SO; **1**·(CH3)2NCHO; **1**·(CH3)2NCOCH3

Results and Discussion

The first section reports the syntheses and characterizations of the three new carceplexes. The second section provides evidence that the shell closures must be templated by their guest molecules and that in so doing exercise structural recognition during the shell closures. The third section describes the crystal structures of cavitand **5** and of **1**·$(CH_3)_2NCOCH_3$. The fourth section reports the ^1H and ^{13}C NMR spectra of the three carceplexes and the degrees of rotational freedom of guest vs host. The fifth section compares the barriers to rotation around the C–N bond of the incarcerated amides with these barriers in the liquid and gas phases. The sixth section addresses the question of whether incarcerated molecules and external molecules or surfaces to the carceplexes communicate with one another. In the seventh section, we interpret the IR spectrum of **1**·$(CH_3)_2NCOCH_3$ in terms of a chiral element in both host and guest. In the last section, the carceplexes' *inner phase* is compared with the interiors of spherands and cryptands, cavitands, zeolites, and clathrates.[5]

Syntheses and Characterization. Octol **3**, reported previously,[6] was prepared from resorcinol and dihydrocinnamaldehyde (69%) and brominated with *N*-bromosuccinimide in 2-butanone to give **4** (58%). Treatment of **4** with CH_2BrCl–K_2CO_3–$(CH_3)_2NCOCH_3$ gave cavitand **5** (52%). This material in tetrahydrofuran (THF) was metalated at −78 °C with *t*-BuLi. The organometallic obtained was quenched with $(CH_3O)_3B$ to form the arylboronic ester, which without isolation was oxidized with H_2O_2–NaOH to produce tetrol **2** (53%) and triol **7** (23%) (Chart I).

The shell closures of **2** to give **1**·G were conducted under high-dilution conditions in purified, dry $(CH_3)_2SO$, $(CH_3)_2NCOCH_3$, or $(CH_3)_2NCHO$ solutions with Cs_2CO_3 as base. To these solutions stirred at 60 °C was added a 3:1 mole mixture of tetrol **2** and CH_2BrCl over 10 h. The reaction mixture was then heated

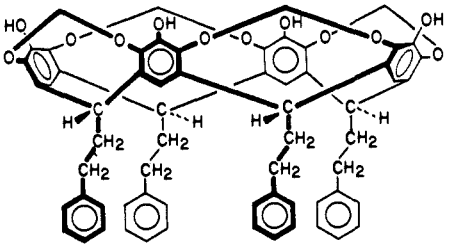

2

to 100 °C for 2 days, during which time a total of 10–15 additional equiv of CH_2BrCl was added in 5–10 portions. The **1**·$(CH_3)_2SO$, **1**·$(CH_3)_2NCOCH_3$, and **1**·$(CH_3)_2NCHO$ formed were purified by chromatography on silica gel ($CHCl_3$–hexane) and crystallized ($CHCl_3$–CH_3CN) to give products in 61, 54, and 49% yields, respectively. Presumably, the ArO^- attacks the CH_2BrCl in an S_N2 reaction to give $ArOCH_2Cl$[7] as an intermediate whose reaction with the second phenoxide is helped by the unshared electron pairs on oxygen.[8] If the reaction mixtures were stirred at 60 °C for 3 days, the desired products were not observed. When the reaction mixtures were stirred for only 1 day at 100 °C, a product was isolated that moved more slowly on the chromatograph and whose ^1H NMR spectrum was consistent with a tris-bridged carcerand containing two unreacted phenolic hydroxyls. This material, when warmed to 100 °C in the corresponding solvent with Cs_2CO_3 and CH_2BrCl, produced the tetrakis-bridged material. This result suggests that introduction of the fourth methylene bridge occurs more slowly than those of the first three bridges. An examination of a Corey–Pauling–Koltun (CPK) molecular model of the tris-bridged diphenol indicates the nucleophilic hydroxyl anions are much more sterically hindered by the bridges already in place than the anions involved in closing the other three bridges.

Elemental analyses of **1**·$(CH_3)_2SO$ for C, H, O, and S and of **1**·$(CH_3)_2NCOCH_3$ and **1**·$(CH_3)_2NCHO$ for C, H, O, and N gave results within 0.20% of theory. The sums for the analyzed elements for each carceplex ranged from 99.73 to 99.90%. Since the carcerands themselves do not contain S or N, these analytical results alone indicate the compounds are 1:1 complexes. These compounds were soluble in $CHCl_3$ (5 mg/mL), slightly soluble in C_6H_6, $CH_3C_6H_5$, CCl_4, CH_2Cl_2, Cl_3CCH_3, $Cl_2CHCHCl_2$, $C_6H_5NO_2$, $(CH_2)_6$, CS_2, and $CH_3(CH_2)_4CH_3$; sparingly soluble in CH_3CN, $(CH_3)_2NCOCH_3$, $(CH_3)_2NCHO$, and $(CH_3)_2SO$; and

(5) Cram, D. J. *Science* **1988**, *240*, 760–767.
(6) Tunstad, L. M.; Tucker, J. A.; Dalcanale, E.; Weiser, J.; Bryant, J. A.; Sherman, J. C.; Helgeson, R. C.; Knobler, C. B.; Cram, D. J. *J. Org. Chem.* **1989**, *54*, 1305–1312.
(7) Pappalardo, S.; Bottino, F.; Tringali, C. *J. Org. Chem.* **1987**, *52*, 405–412.
(8) Summers, L. *Chem. Rev.* **1955**, *55*, 301–353.

Chart II

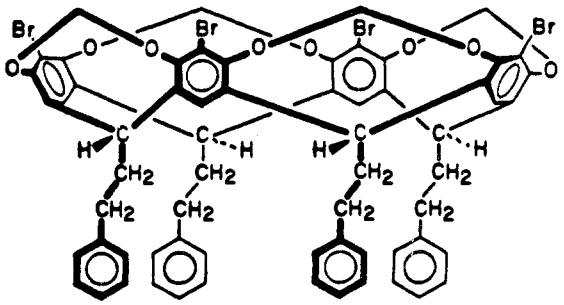

5

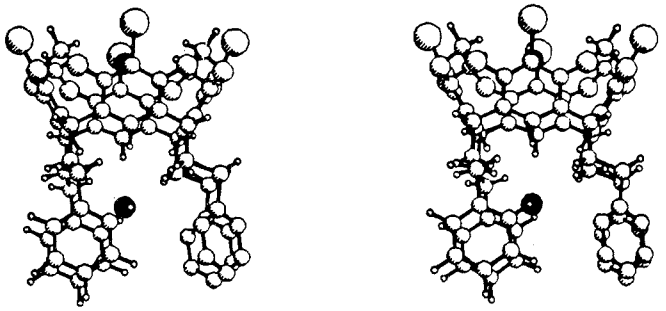

5•2H2O crystal structure (O's of H2O darkened)

insoluble in H_2O, CH_3OH, and C_2H_5OH.

When heated to reflux for 12 h, a solution of $\mathbf{1}\cdot(CH_3)_2SO$ in $(CH_3)_2NCHO$ failed to undergo guest exchange. We conclude that the guests are trapped inside their molecular prisons and can depart only by bond-breaking processes.

The carceplexes were submitted to three types of MS determinations. Samples of $\mathbf{1}\cdot(CH_3)_2NCOCH_3$ and $\mathbf{1}\cdot(CH_3)_2NCHO$ were each prepared by adding their $CHCl_3$ solutions to 3-$NO_2C_6H_4CH_2OH$, evaporating the $CHCl_3$, and submitting the samples to fast atom bombardment (FAB) with xenon.[9] The parent peak (m^{2+}/z = 936) corresponded to $\mathbf{1}^{2+} - C_6H_5CH_2CH_2$ (100%); 1041, $\mathbf{1}^{2+}$ (90%); 2082, $\mathbf{1} + H^+$ (10%); 2169, $\mathbf{1}\cdot(CH_3)_2NCOCH_3 + H^+$ (20%); and 2155, $\mathbf{1}\cdot(CH_3)_2NCHO + H^+$ (30%). Many other peaks were also present that corresponded to **1** minus one or three CH_2 groups with or without loss of $C_6H_5CH_2CH_2$ groups. In the FAB mode, no strong signals were observed. Obviously, the carceplexes are fragmented by the high-energy xenon atoms.[10]

All three carceplexes mixed with NaCl were subjected to laser desorption Fourier transform mass spectrometry (LD FTMS).[11,12] Only weak signals were detected in the negative mode. In the positive mode, good signals (m/z) were observed: for $\mathbf{1}\cdot(CH_3)_2SO + Na^+$, 2181.7 (100%); $\mathbf{1} + Na^+$, 2103.7 (25%); $\mathbf{1} - CH_2 + 2H + Na^+$, 2091.7 (10%); for $\mathbf{1}\cdot(CH_3)_2NCOCH_3 + Na^+$, 2190.8 (50%); $\mathbf{1} + Na^+$, 2103.7 (100%); $\mathbf{1} - CH_2CH_2C_6H_5 - H + Na^+$, 1997.7 (30%); $\mathbf{1} - 2\,CH_2 + Na^+$, 2075.7 (25%); for $\mathbf{1}(CH_3)_2NCHO + Na^+$, 2176.7 (100%); $\mathbf{1} + Na^+$, 2103.7 (100%); $\mathbf{1} - C_6H_5CH_2CH_2 - H + Na^+$, 1997.6 (40%); $\mathbf{1} - 2\,CH_2 + Na^+$, 2075.7 (20%). No signals were observed with m/z higher than $\mathbf{1}\cdot G + Na^+$ or between $\mathbf{1} + Na^+$ and $\mathbf{1}\cdot G + Na^+$. Laser desorption–photodissociation experiments[13] on each carceplex demonstrated that the $\mathbf{1}\cdot G + Na^+$ ions degraded to $\mathbf{1} + Na^+$ species, undoubtedly by processes that involve covalent bond breaking.

The three carceplexes were subjected to desorption chemical ionization[14] mass spectrometry (DCI MS) by use of a thin filament coated with sample heated very rapidly (2.5 s) with $(CH_3)_3CH$ as the reagent gas.[15] Both $\mathbf{1}\cdot(CH_3)_2SO$ and $\mathbf{1}\cdot(CH_3)_2NCHO$ gave m/z ions for $\mathbf{1}\cdot G^+$ (100%) and $\mathbf{1}^+$ (5%), whereas $\mathbf{1}\cdot(CH_3)_2NCOCH_3$ gave m/z ions for $\mathbf{1}\cdot G^+$ (60%) and $\mathbf{1}^+$ (100%). A 12.5-s heating time gave greatly increased signals for $\mathbf{1}^+$ relative to $\mathbf{1}\cdot G^+$ compared to the shorter heating time. These data taken in sum indicate that the three carceplexes possess structures in which one molecule of solvent is incarcerated during each shell closure and that no carcerand (without guest) is made.

Template Effect Coupled with Structural Recognition in Shell Closures. To determine whether empty carcerand **1** could be prepared, tetrol **2** was submitted to the same kind of shell-closure conditions employed for the carceplex formations except that $CH_2(CH_2CH_2)_2NCHO$ was used as solvent. This compound in CPK models is too large to be enclosed by a model of **1** without incurring great strain. The reaction yielded only polymeric materials, even after the final reaction mixture had been heated to 150 °C. Another reaction was conducted under normal conditions in a 0.5 mol % $(CH_3)_2NCOCH_3$ solution in $(CH_2)_5NCHO$, which provided 50 equiv of $(CH_3)_2NCOCH_3$ per potential carcerand. A 10% yield of $\mathbf{1}\cdot(CH_3)_2NCOCH_3$ was produced. Thus, it appears that a shell closure that encloses only empty space cannot occur.

We interpret this as follows. The nucleophilic substitution reactions of the shell closures and competing polymerizations involve phenoxides as nucleophiles, which require solvation of the negative charge. When the solvating molecules are too large to fit into the cavity of the product-determining transition state, only polymerization occurs because the reacting groups are held too far apart for shell-closing reactions by the partially enclosed solvent that fills the cavitand parts. That the cavitand parts should contain empty space is unlikely on entropic grounds. Organic liquids are only ~30% empty space,[16] which is broken into small volumes between molecules that inefficiently contact one another because of their shapes. The gathering together of many small volumes to create two empty cavitands that then undergo multiple reactions with one another must overcome the entropy of dilution of these small volumes.

A competition experiment was performed by conducting a standard shell closure in a 1:1 molar ratio of $(CH_3)_2NCOCH_3$ and $(CH_3)_2NCHO$. A 5:1 ratio of $\mathbf{1}\cdot(CH_3)_2NCOCH_3$ to $\mathbf{1}\cdot(CH_3)_2NCHO$ was produced in a collective 27% yield. In a second run, a 1:6 molar ratio of $(CH_3)_2NCOCH_3$ and $(CH_3)_2NCHO$ was employed to give a 1:1 ratio of $\mathbf{1}\cdot(CH_3)_2NCOCH_3$ to $\mathbf{1}\cdot(CH_3)_2NCHO$ in a collective yield of 20%.

We interpret this factor of 5 in structural recognition of the larger of the two amide guests as reflecting the relative complementarity of the two amides to the product-determining transition state. This transition state must occur after one bridge is in place and during the reaction that completes the second or third bridge. Molecular model (CPK) examination indicates that once two anti bridges are in place, neither amide can easily escape the interior of the shell. The hydrogen-bonded interhemispheric hydroxyls and the intrahemispheric methylenes block the way. The volume

(9) We warmly thank Dr. Sensharma of our department for running these FABMS.

(10) Silverstein, R. M.; Bassler, G. C.; Morrill, T. C. *Spectroscopic Identification of Organic Compounds*; John Wiley: New York, 1981; p 23.

(11) Ijames, C. F.; Wilkins, C. L. *J. Am. Chem. Soc.* **1988**, *110*, 2687–2688.

(12) We warmly thank C. Yung and Dr. C. L. Wilkins for performing these laser desorption experiments.

(13) Hahn, J. H.; Zenobi, R.; Zare, R. N. *J. Am. Chem. Soc.* **1987**, *109*, 2842, 2843.

(14) Beaugrand, C.; Devant, G. *Adv. Mass Spectrom.* **1980**, *8B*, 1806–1811.

(15) We thank Dr. G. Guglielmetti for carrying out the DCI MS experiments.

(16) We thank Dr. Raymond A. Firestone for the following references and for a discussion of this question. (a) Reichardt, C. *Solvents and Solvent Effects in Organic Chemistry*; Verlag Chemie: New York, 1988; p 5. (b) Cameron, C.; Saluja, P. P. S.; Floriano, M. A.; Whalley, E. *J. Phys. Chem.* **1988**, *92*, 3417–3421. (c) Reichardt, C. *Ibid.* p 280. (d) Asano, T.; le Noble, W. *Rev. Phys. Chem. Jpn.* **1973**, *43*, 82–91. (e) Nishimura, N.; Tanuka, T.; Motoyama, J. T. *Can. J. Chem.* **1987**, *65*, 2248–2253. (f) Firestone, R. A.; Smith, G. *Chem. Ber.* **1989**, *122*, 1089–1094. (g) Markus, Y. *Introduction to Liquid State Chemistry*; Wiley: New York, 1977; p 58.

Chart III

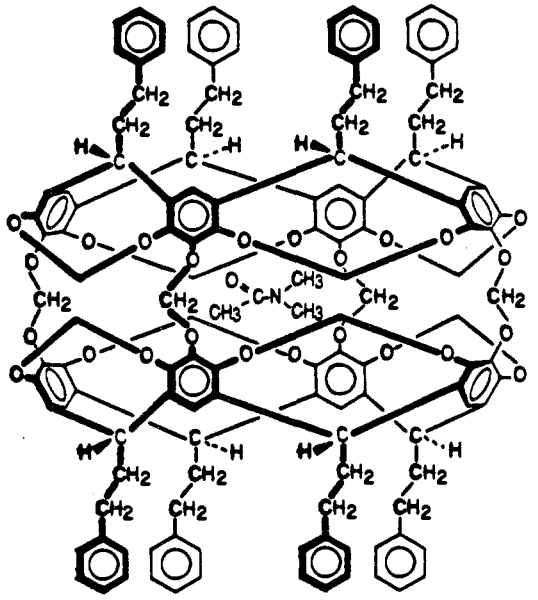

1•$(CH_3)_2NCOCH_3$

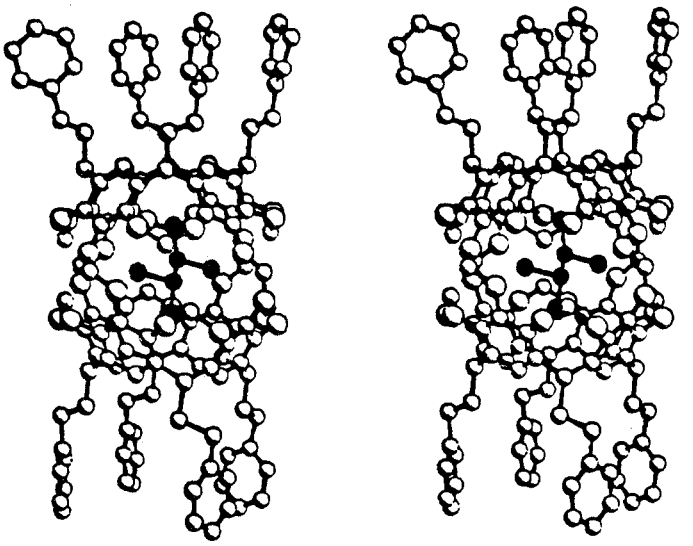

1•$(CH_3)_2NCOCH_3$ side view (guest darkened)

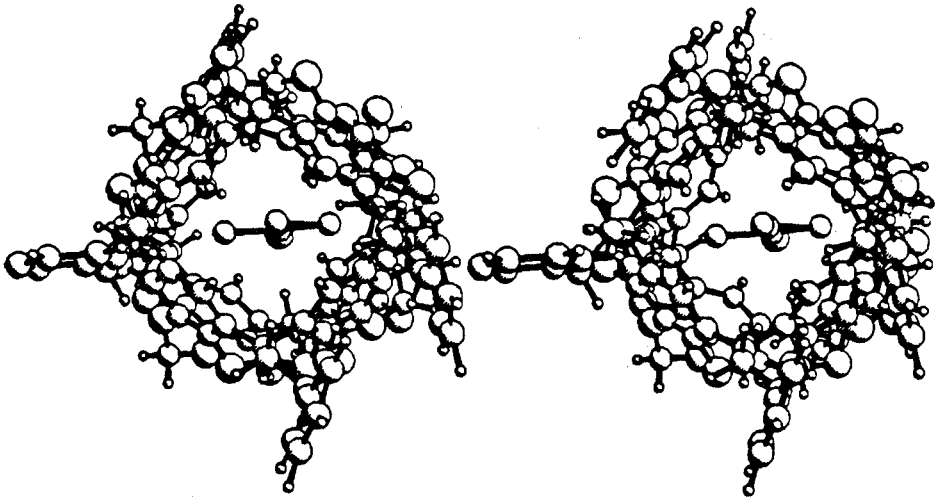

1•$(CH_3)_2NCOCH_3$ end view

of this transition state in models is larger than that of the final carcerand, and $(CH_3)_2NCOCH_3$ has more complementary contacts with the shell parts than the smaller $(CH_3)_2NCHO$. These facts indicate the operation of structural recognition through a more or less efficient template effect during shell closure.

Crystal Structures of Caviplex 5·2H_2O and Carceplex 1·$(CH_3)_2NCOCH_3$. The crystal structure of caviplex 5·2H_2O was determined (R = 0.074). One water was found as a guest in the bowl and a second occupied a position in between the four $C_6H_5CH_2CH_2$ groups. These cavitands are packed head to tail in the crystal. Two of the pendant phenyl groups are ordered, whereas the other two have two equally populated positions, only one set of which is formulated in the stereoview of 5·2H_2O, which is drawn (Chart II). The dimensions of the bowl part of the caviplex are close to those observed for 6·$CHCl_3$ reported earlier.[17] Table I provides the bond angles, bond distances, and other structural parameters defined by general diagram **8** and footnote *a* of the table. The parameters of 6·$CHCl_3$ are included in Table I for comparison. Thus, the replacement of the four pendant CH_3 groups in **6** by four pendant $CH_2CH_2C_6H_5$ groups in **5** or the change in guest in the cavity from $CHCl_3$ of **6** to H_2O in **5** have only small effects on the bowl dimensions.

The crystal structure of carceplex 1·$(CH_3)_2NCOCH_3$·5$CHCl_3$ was also determined (R = 0.184). Both side and end stereoviews are depicted (the five $CHCl_3$'s are omitted). In the side views, the six heavy atoms of the $(CH_3)_2NCOCH_3$ guest are darkened. The dimensions of the bowl portions in the crystal structure of 1·$(CH_3)_2NCOCH_3$ are very similar to those of 5·H_2O and **6**, so the attachment of two bowls together with four OCH_2O bridges has comparably small effects on the shapes and volumes of the bowl parts of the carceplex (Chart III).

An important feature of the crystal structure is that the northern hemisphere is rotated around its long polar axis with respect to the southern hemisphere. This axis is not quite linear, because planes "a" (diagram **8**) for the two cavitand moieties are not quite parallel. The two a planes deviate from being parallel by 5.2° and the two b planes by a value of 4.2°. This small tilt and rotation

(17) Cram, D. J.; Karbach, S.; Kim, H.-E.; Knobler, C. B.; Maverick, E. F.; Ericson, J. L.; Helgeson, R. C. *J. Am. Chem. Soc.* **1988**, *110*, 2229–2237.

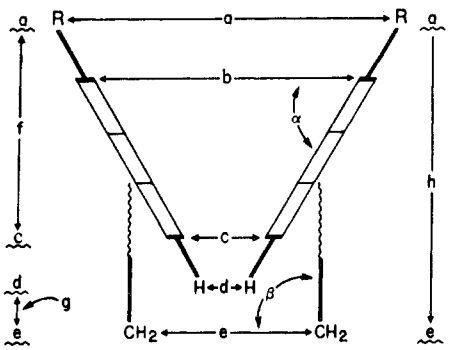

8

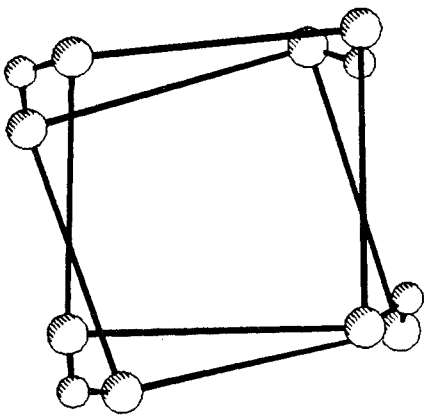

9

are visible in diagram **9** in which the four OCH_2O bridging groups are drawn. In **9**, the four oxygens of the northern hemisphere are connected to one another to form a *near square* and the four oxygens of the southern hemisphere are likewise connected to form a second *near square*. These "squares" are rotated by roughly 25° with respect to one another. Notice that the oxygen's unshared electron pairs and the two hydrogens of the attached CH_2 interhemispheric groups generally face along the surface of the shell or outward, but not inward. These rotations, tilts, and spacial dispositions accommodate the incarcerated guest's volume and shape and also allow the rims of the two hemispheres to pack against each other efficiently to provide close $CH_2O \cdot H_2C$ contacts. The rotation and tilt also destroy the five planes of symmetry of the carcerand portion of the complex, resulting in a chiral shell. The D_4 symmetry with a C_4 long polar axis and four C_2 (short equatorial) axes is left approximately intact. The cavity itself is shaped like a U.S. football, whose long axis is 10.9 Å (distance between two d planes of **8**) and whose short equatorial axis is 6.2 Å (limiting distance between opposite bridging oxygens, or 9 Å–2.8 Å).

The most important structural feature of the crystal structure is that it unequivocably demonstrates that $(CH_3)_2NCOCH_3$ is incarcerated and has no chance of departing the interior without breaking bonds. This conclusion is intuitively obvious by examining the side and end views of **1**·$(CH_3)_2NCOCH_3$. All hydrogens are omitted from both host and guest in the side view and from those of the guest only in the end view. The six heavy atoms (non-hydrogen) of the guest are close to being coplanar. The end view resembles an airplane floating in a wind tunnel. The two (polar) ends of the carcerand **1** have the largest pores in the shell, and each is defined roughly as a circle of four hydrogens (Ar–H) with a diameter of 4.2 Å, which leaves an opening of about 3.2 Å in diameter. There is no way for the doubly branched guest containing six heavy atoms and nine hydrogens to escape through these small holes.

Although the guest **10** is not well defined crystallographically, we have located its six non-hydrogen atoms. They are roughly coplanar. We have not distinguished between the oxygen and the carbonyl's methyl with certainty. CH_3 group a attached to the

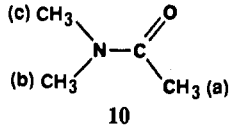

10

carbonyl group of **10** is close to being centered in the temperate zone of the northern hemisphere, whereas the c CH_3 group attached to nitrogen and anti to CH_3 occupies a comparable place in the southern hemisphere. The b CH_3 group is in the torrid zone slightly north of the equator, whereas the carbonyl oxygen is located in the torrid zone slightly south of the equator. The long axis of the guest passes through the a CH_3 and the c CH_3, and this axis is close to being coincident with the long (polar) axis of the cavity. Although much of the cavity of carcerand **1** is filled with the $(CH_3)_2NCOCH_3$ molecule, some empty space flanks the rough plane of the guest and is found in the polar regions. In the crystal, much of the space between the carcerands is filled with solvent $CHCl_3$ molecules. Most of these are disordered. Although only five such molecules have been located, there are indications that more solvent is present.

Chart IV. Proton and Carbon Identification (Eye Is Inside Looking Outward)

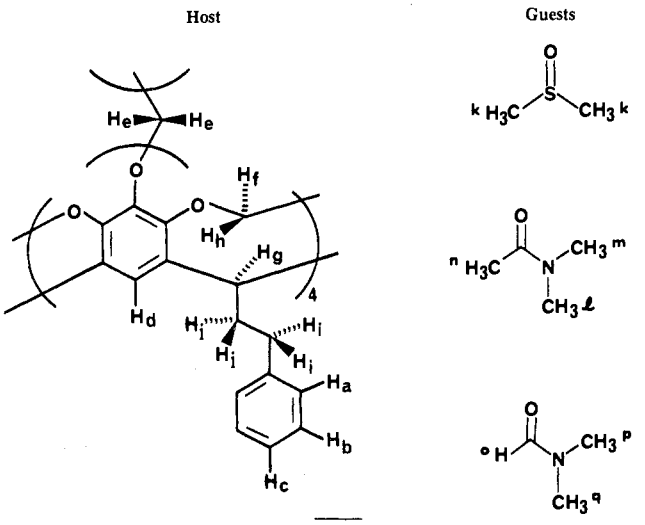

The fact that the guest $(CH_3)_2NCOCH_3$ molecules in the crystal of **1**·$(CH_3)_2NCOCH_3$ are largely ordered (except with respect to $(CH_3)_2N$ and $COCH_3$ interchanging their positions) shows that each guest in effect communicates its rotational position around its long axis to guests in neighboring carceplex molecules. This structural recognition feature might be due to subtle host deformations caused by the relatively large space requirements of the guest.

A minimum energy MM2 calculation of a symmetrized structure of carceplex **1**·$(CH_3)_2NCOCH_3$ (the eight pendant $CH_2CH_2C_6H_5$ groups are replaced by eight hydrogens) is drawn in **11** (oxygens are shaded, and the northern hemisphere is not twisted relative to the southern hemisphere)[18] and corresponds roughly to what was observed in the crystal structure, which in turn corresponds closely to a CPK molecular model of **11**.

^{1}H NMR Spectra. The 360-MHz ^{1}H NMR spectral data of **1**·$(CH_3)_2SO$, **1**·$(CH_3)_2NCOCH_3$, and **1**·$(CH_3)_2NCHO$ are recorded in Table II, and Chart IV identifies the assignments of chemical shifts to the protons. The assignments of protons a–c and f–j were derived from the analogous resonances in the $CHCl_3$ ^{1}H NMR spectrum of the bowl-shaped cavitand, **5** (see Experimental Section). The assignments of protons d and e were derived from heteronuclear decoupling experiments employing **1**·$(CH_3)_2NCHO$ as follows. With no irradiation, the ^{13}C NMR spectrum provided triplets at 90 and 103 ppm, which are due to

(18) We thank Drs. K. N. Houk, A. E. Dorigo, and B. Thomas for carrying out these calculations, which were made before the crystal structure was available. Details of new calculations based on the helical model will be published elsewhere.

Table I. Distances and Angles Relevant to the Shapes of Cavities and Derived Carceplex[a]

cryst struct param	**5**·2H_2O	**6**·$CHCl_3$	**1**·$(CH_3)_2NCOCH_3$·5$CHCl_3$	
			northern hemis	southern hemis
	Distances (Å)			
R···R diagonal of plane a (*a*)	9.45, 9.68	9.34, 9.81	9.47, 8.94	9.51, 8.84
$(R\cdots R)_{av}$ for a	9.56	9.58	9.20	9.18
R out of plane a	±0.03	±0.06	±0.13	±0.13
C···C diagonal of plane b (*b*)	7.94, 7.78	8.00, 7.83	8.03, 7.76	8.12, 7.69
$(C\cdots C)_{av}$ for b	7.86	7.92	7.90	7.91
C out of plane b	±0.01	±0.02	±0.11	±0.07
C···C diagonal of c (*c*)	5.25, 5.22	5.25, 5.23	5.27, 5.25	5.25, 5.25
$(C\cdots C)_{av}$ for c	5.24	5.24	5.24	5.25
C out of plane c	±0.02	±0.02	±0.05	±0.05
H···H diagonal of plane d (*d*)	4.2, 4.1	4.29, 4.26	4.3, 4.2	4.2, 4.1
$(H\cdots H)_{av}$ for d	4.2	4.28	4.3	4.2
H out of plane d	±0.0	±0.02	0.0	0.0
$CH_2\cdots CH_2$ diagonal of plane e (*e*)	7.13, 7.13	7.34, 7.02	7.42, 7.28	7.24, 7.13
$(CH_2\cdots CH_2)_{av}$ for e	7.13	7.18	7.35	7.18
CH_2 out of plane e	±0.0	±0.08	±0.04	±0.04
plane a to c (*f*)	4.1	4.15	3.6	3.6
plane d to e (*g*)	0.6	0.67	0.6	0.7
plane a to e (*h*)	5.7	5.69	5.2	5.2
near O···O	2.33, 2.36	2.33, 2.42	2.34, 2.43	2.38, 2.37
		2.34, 2.31	2.36, 2.33	2.36, 2.39
near $(O\cdots O)_{av}$	2.34	2.35	2.36	2.38
	Angles (deg)			
planes a and c		0.5	0.7	1.9
planes d and e	0.0	1.0	1.5	1.8
planes a and e	0.3	0.7	0.6	0.8
planes benzene and b (α)	0.1	60.9, 62.8	59.4, 63.0	59.0, 62.6
	60.5, 62.2	59.9, 61.0	59.0, 62.5	63.1, 58.9
α_{av}	61.3, 62.2	61.2	61.0	60.6
plane e to CH_2C (β)	61.6	85.8, 85.2	85.9, 88.6	83.8, 86.3
	76.9, 76.7	87.7, 86.3	85.6, 82.3	81.7, 86.0
β_{av}	77.0, 76.8	86.2	85.6	84.4
	76.8			

[a] Planes a–e are defined as the best planes in general diagram **8** of the following: a, four R groups; b, four aryl carbons bonded to R groups; c, four aryl carbons bonded to hydrogen; d, four aryl hydrogens; and e, four aryl methylenes. Distances *a*–*e* (Å) refer to atoms in planes most distant from one another in the respective a–e planes. Distances f and g are those between best planes. Diagram **8** in the text explicitly defines the distances and angles. Data taken from Table II of ref 17.

Table II. Carcerands' ^1H NMR Spectral Data in $CDCl_3$ at Ambient Temperature

protons[a]	description[b]	δ[c] of carceplex		
		1·$(CH_3)_2SO$	**1**·$(CH_3)_2NCOCH_3$	**1**·$(CH_3)_2NCHO$
$H_{a,b,c}$	m, 40 H	7.12–7.24	7.12–7.23	7.12–7.23
H_d	s, 8 H	6.76	6.74	6.78
H_e	s, 8 H	6.57	6.51	6.55
H_f	d, 8 H, J = 7.5	6.16		6.12
H_f	m, 8 H		6.08	
H_g	t, 8 H, J = 7.8	4.88		4.89
H_g	t, 8 H, J = 7.5		4.91	
H_h	d, 8 H, J = 7.5	4.49		4.50
H_h	d, 8 H, J = 7.1		4.64	
H_i	m, 16 H	2.63	2.65	2.63
H_j	m, 16 H	2.46	2.46	2.46
H_k	s, 6 H	−1.24		
H_l	s, 3 H		1.04	
H_m	s, 3 H		−1.46	
H_n	s, 3 H		−2.40	
H_o	s, 1 H			4.28
H_p	s, 3 H			−0.04
H_q	s, 3 H			−1.02

[a] See Chart IV for identification. [b] J in hertz. [c] $(CH_3)_4Si$, δ 0.

the two acetal carbons. A doublet at 113 ppm corresponds to the carbon attached to H_d. Upon irradiation of the proton resonance at 6.55 ppm only, the triplet at 90 ppm collapsed to a singlet, showing that H_e is in fact at 6.55 ppm and that the interhemisphere acetal carbon's signal is at 90 ppm while that of the intrahemisphere carbon is at 103 ppm.

The assignments of the guest protons are as follows. The resonances of these protons are all dramatically shifted upfield, which is consistent with their locations within the carcerand in close proximiity to the shielding zone of the arenes.[24] To be sure that the guests were not merely complexed to the pendant phenylethyl groups, control experiments were performed. The ^1H NMR spectra of bowl-shaped cavitand **5** in $CDCl_3$ with 1 equiv of $(CH_3)_2SO$, $(CH_3)_2NCOCH_3$, or $(CH_3)_2NCHO$ each showed no changes in the proton spectra of these guests relative to the spectra of these guests each alone in $CDCl_3$. Furthermore, no change was observed in the ^1H NMR spectra of any of the three carceplexes when each was heated at 135 °C for 24 h at 10^{-5} Torr. When $C_6D_5NO_2$ solutions of **1**·$(CH_3)_2NCOCH_3$ and **1**·$(CH_3)_2NCHO$ were each heated to over 160 °C and then cooled, their ^1H NMR spectra remained unchanged. Thus, the guests are truly incarcerated, for they can be neither washed nor evaporated away from the host.

Careful integrations[19] of the guest protons against the host

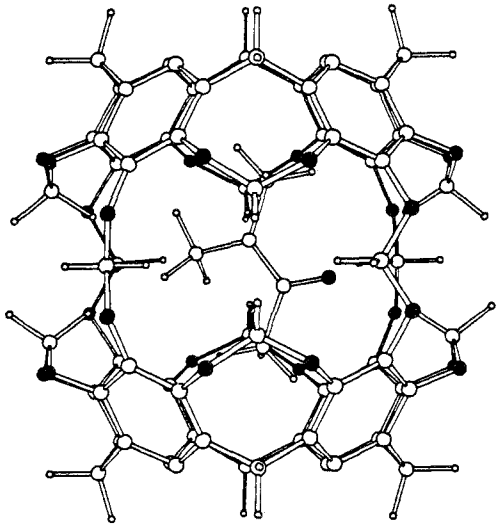

11

protons indicated the host to guest ratios to be 1:1 within 2–5% error.[20] *The results from the elemental analyses, mass and ^1H NMR spectra, and a crystal structure taken together leave no doubt that the guests are incarcerated.*

The crystal structure, MM2 calculations, and CPK molecular model examinations all indicate that the long axis of the $(CH_3)_2NCOCH_3$ molecule is roughly coincident with the long axis of **1** in **1**·$(CH_3)_2NCOCH_3$. This long axis is defined by the acetyl methyl and the *N*-methyl that is syn to the carbonyl group. The dynamic ^1H NMR experiments described in a later section demonstrate that the two *N*-methyl groups generate the two signals at δ −1.46 and 1.04. We assign the H_m protons of the *syn*-methyl to the more aryl-shielded upfield chemical shift at δ −1.46 and the H_l protons of the *anti*-methyl to the less aryl-shielded upfield chemical shift at δ 1.04. The incarcerated H_m protons are shifted δ 4.40 upfield from their normal position in $CDCl_3$, while the incarcerated H_l protons are shifted δ 1.98 from their normal position in $CDCl_3$.[21] The H_n protons of the acetyl group give a signal at δ −2.40 and are shifted δ 4.49 upfield from their normal position in $CDCl_3$.[21] Thus, the two methyls (H_m and H_n) on the longest axis of the $(CH_3)_2NCOCH_3$ guest are pushed into the high-shielding temperate zones of the northern and southern hemispheres, whereas the third methyl is in the torrid zone close to the equator, which is less shielding.

Carcerand **1** possesses an equatorial array of eight H_h protons that line the torrid region close to the guest H_l protons in **1**·$(CH_3)_2NCOCH_3$. Nuclear Overhauser enhancement (NOE) experiments[22] were performed to see if irradiation of the host's H_h protons would enhance the H_l protons of the guest. In fact, the resonance at δ 1.04 was enhanced by a modest 3%, whereas no enhancement was observed for the other guest protons. This solution experiment confirms the expectations based on the crystal structure of **1**·$(CH_3)_2NCOCH_3$.

Drawing **12** represents the MM2-calculated minimum energy structure for **1**·$(CH_3)_2NCHO$ in which eight hydrogens replace the eight $CH_2CH_2C_6H_5$ groups (oxygens are shaded, and no twisted forms were calculated). Notice that the *N*-CH_3 anti to the oxygen extends well into the northern temperate shielding zone of the host, whereas the *N*-CH_3 syn to the carbonyl is located in the less shielding southern torrid zone. Accordingly, the ^1H NMR signal at δ −1.02 is assigned to the anti (H_a) protons, which are δ 4.00 upfield of these proton signals of $(CH_3)_2NCHO$ dissolved in $CDCl_3$.[21] The protons (H_p) of the *N*-CH_3 syn to the carbonyl group are assigned to the signal at δ −0.04, which is shifted δ 2.90 upfield of these proton signals of $(CH_3)_2NCHO$ dissolved in $CDCl_3$.[21] The aldehydic proton (H_o) of **1**·$(CH_3)_2NCHO$ occurs at δ 4.28, which is δ 3.77 upfield of its normal chemical shift in $CDCl_3$.[21] In **12**, this proton is located north of the equator but still in the torrid zone. Thus, the ^1H NMR spectrum of **1**·$(CH_3)_2NCHO$ is in reasonable agreement with the MM2-calculated structure.

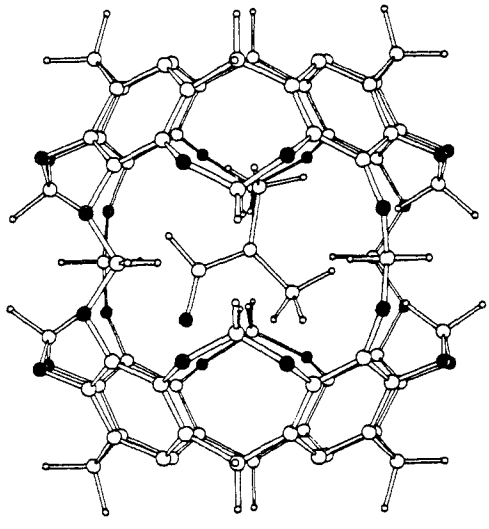

12

Drawing **13** portrays the MM2-calculated minimum energy structure for **1**·$(CH_3)_2SO$ in which eight hydrogens replace the eight $CH_2CH_2C_6H_5$ groups (oxygens are shaded, and no twist forms were calculated). Notice that the two methyl groups are located not quite symmetrically in the northern and southern hemispheres, partly in the temperate and partly in the torrid zones, close to where the *N*-CH_3 (H_n) anti to carbonyl group resides in drawing **12** of **1**·$(CH_3)_2NCHO$. The oxygen of the S → O group is slightly south of the equatorial band of four interhemispheric CH_2O groups in **13**. The ^1H NMR spectrum of the guest of **1**·$(CH_3)_2SO$ at ambient temperature exhibits only one kind of proton (H_k) at δ −1.24 which is δ 3.86 upfield of these proton signals for $(CH_3)_2SO$ dissolved in $CDCl_3$.[23] This upfield shift is close to that (δ 4.00) for the H_p proton in **1**·$(CH_3)_2NCHO$.

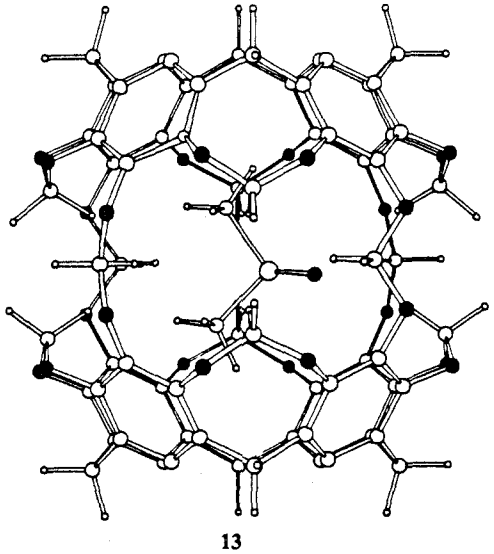

13

The chemical shifts of the protons of the host common to the three carceplexes are very similar to one another (see Table I) except for H_h and H_f (respective inward- and outward-turned protons of intrahemispheric OCH_2O bridges). The shifts and multiplicities for these proton signals are different for **1**·$(CH_3)_2NCOCH_3$ than for **1**·$(CH_3)_2SO$ or **1**·$(CH_3)_2NCHO$, which are similar to one another. Thus, H_h and H_f of **1**·$(CH_3)_2NCOCH_3$

(19) We thank N. Jaffer for his assistance in obtaining accurate integration. The acquisition time was 4.0 s, the relaxation delay was 5.0 s, the pulse angle was 30°, and the samples were degassed.

(20) Herring, F. G.; Phillips, P. S. *J. Magn. Reson.* **1985**, *62*, 19–28.

(21) Lewin, A. H.; Frucht, M. *Org. Magn. Reson.* **1975**, *7*, 206–225.

(22) We warmly thank M. Geckle for his assistance with the NOE and ^{13}C NMR experiments.

(23) *Handbook of Proton-NMR Spectra and Data*; Asahi Research Center, Ed.; Academic Press: Tokyo, 1985; p 1, 39.

Table III. Partial ^{13}C NMR Spectra Structural Assignments to the Host of the Three **1**·G Carceplexes in $CDCl_3$

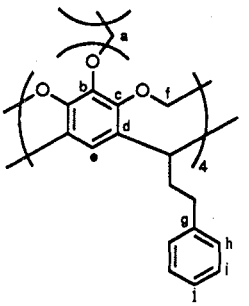

assignment	obsd chem shift (δ) **1**·$(CH_3)_2SO$	**1**·$(CH_3)_2NCHO$	**1**·$(CH_3)_2NCOCH_3$	calcd chem shift (δ)
b, c, or d	144	143.8	144.2/144	130 (b)
b, c, or d	141.5	141.5	141.9/141.7	123 (d)
b, c, or d	141.2	141.1	141.53/141.47	143 (c)
g	139.6	139.7	139.3	145
h or i	128.6	128.6	128.6	130
h or i	128.4	128.4	128.4	130
j	126.1	126.1	126.1	130
e	112.4	112.7	113.1	115
f	102.1	101.6	101.0/100.7	90
a	91.3	91.4	95.3	90

occur as a doublet and multiplets at δ 4.64 and 6.08, respectively, whereas H_h and H_f of **1**·$(CH_3)_2NCHO$ both occur as doublets at δ 4.50 and 6.12. These results imply that the more voluminous $(CH_3)_2NCOCH_3$ guest stereoelectronically affects the northern and southern hemispheres differently by providing different environments for the inward-turned H_f protons in the two hemispheres, which in turn suggests that the $(CH_3)_2NCOCH_3$ molecule, while rotating rapidly (on the ^1H NMR time scale) around the long C_4 axes of the host, is rotating slowly or not at all around the short C_2 axes. The simpler ^1H NMR spectra of **1**·$(CH_3)_2NCHO$ and **1**·$(CH_3)_2SO$ suggest these molecules are rapidly rotating around both the C_2 and C_4 axes, providing both the northern and southern hemispheres with the same averaged environments. Molecular model (CPK) examinations are consistent with these interpretations.

^{13}C NMR Spectra. Table III records the calculated[24] and observed ^{13}C NMR chemical shifts in $CDCl_3$ for the hosts of **1**·$(CH_3)_2SO$, **1**·$(CH_3)_2NCHO$, and **1**·$(CH_3)_2NCOCH_3$ along with their structural assignments. INEPT experiments[22] were performed in order to determine the multiplicity of each carbon. The signals at δ 128.6, 128.4, 126.1, and 112.4 were found to be CH groups and were further assigned in Table II on the basis of their predicted chemical shifts. Carbon C_j was differentiated from C_h and C_i on the basis of the lower intensity of the δ 126.1 resonance (eight C_j carbons) compared to those of C_h and C_i (16 carbons of each). Resonances at δ 102.1 and 91.3 were determined to be CH_2 groups and were identified by the proton H_e irradiation experiment described earlier. The carbon resonance at δ 139.6 was assigned to C_g on the basis of the calculated chemical shift and the near identity of this resonance (δ 139.6, 139.7, and 139.3) for the three carceplexes. This carbon is too remote from the guest to be affected by its character. The resonances at δ 144, 141.5, and 141.2 were assigned to C_b, C_c, and C_d in unknown order on the basis of the perturbation with $(CH_3)_2NCOCH_3$ as the guest in comparison to $(CH_3)_2SO$ or $(CH_3)_2NCHO$ as guest, since these carbons line the cavity of the shell. It is not clear why C_b and C_d appear so far from their calculated chemical shifts.[24]

Table III clearly shows that $(CH_3)_2NCOCH_3$ as guest reduces the symmetry of the carcerand host, whereas $(CH_3)_2SO$ and $(CH_3)_2NCHO$ do not. Thus, C_b, C_c, C_d, and C_f signals are split in the spectrum of **1**·$(CH_3)_2NCOCH_3$ but are clear singlets in those of **1**·$(CH_3)_2SO$ and **1**·$(CH_3)_2NCHO$. Similarly, H_f and H_h are not as symmetrical in **1**·$(CH_3)_2NCOCH_3$ as they are in **1**·$(CH_3)_2SO$ and **1**·$(CH_3)_2NCHO$. The splittings of H_f, H_h (^1H NMR), C_b, C_c, C_d, and C_f in the $(CH_3)_2NCOCH_3$-occupied host are likely to be due to restricted molecular rotation of this guest relative to its shell. If this restricted rotation was about the long (C_4) axis of the shell, H_e and C_a would be split but they are not. However, if the restricted rotation was about the short C_2 axes, signals of H_f, H_h, C_b, C_c, C_d, and C_f should be split, as was observed. The fact that C_e is not split (as is possible) is consistent with its being too remote from the guest to have its magnetic field altered by which end of the guest was the more proximate.

Temperature-Dependent ^1H NMR Spectra. In $C_6D_5NO_2$ as solvent, the H_f and H_h protons of the shell of **1**·$(CH_3)_2NCOCH_3$ did not become a clear AB quartet up to 175 °C. Thus, even at that temperature, the guest did not rotate around the C_2 axes of the shell.

In $CDCl_3$, the ^1H NMR spectrum of **1**·$(CH_3)_2NCHO$ did not change with changes in temperature down to 235 K. However, in $CDCl_3$ the ^1H NMR spectrum of **1**·$(CH_3)_2SO$ below 275 K provides two signals for the guest protons at δ −1.27 and −1.38 (360 MHz) and below 255 K provides two doublets for the H_h host protons at δ 4.46 and 4.37. This suggests that the rotation of $(CH_3)_2SO$ within the shell is constrained enough on the ^1H NMR time scale to relegate one methyl and the sulfur oxygen to one hemisphere (e.g., the southern hemisphere as in **13**) and the other methyl to the other hemisphere (e.g., the northern hemisphere as in **13**). From the difference between the chemical shifts of the two shell H_h protons and the two $(CH_3)_2SO$ methyl protons at low temperature, energy barriers to rotation of the guest about the short C_2 axes were calculated[25] to be $\Delta G^{\ddagger}_{255K}$ = 12.7 and $\Delta G^{\dagger}_{275K}$ = 13.6 kcal mol^{-1}, respectively. In the crystal structure of **1**·$(CH_3)_2NCOCH_3$, the northern hemisphere was rotated about 15° with respect to the southern hemisphere. This rotation probably extends to **1**·$(CH_3)_2SO$ as well. If so, the transition occurring at 255 K may reflect the freezing out (slow on the ^1H NMR time scale) of equilibrations between the directions of rotations of the northern relative to the southern hemispheres, which may occur once the guests' motions are constrained. Why these two transitions occur in **1**·$(CH_3)_2SO$ and not in **1**·$(CH_3)_2NCHO$ must be related to differences in the shapes and possibly the conformational adaptability of the guests.

The C–N Rotational Barrier of the Amide Guests. Dynamic ^1H NMR experiments were performed to compare the energy barrier to C–N rotation of incarcerated and nonincarcerated amide guests in $C_6D_5NO_2$ as solvent. The coalescence of the two *N*-methyl resonances of $(CH_3)_2NCHO$ inside carcerand **1** occurred at 140 °C and provided a $\Delta G^{\dagger}_{413K}$ = 18.9 kcal mol^{-1}.[25] The

(24) See ref 10, pp 260–266.

(25) Atta-ur-Rahman. *Nuclear Magnetic Resonance*; Springer-Verlag: New York, 1986; pp 131–133.

coalescence temperature of $(CH_3)_2NCHO$ dissolved directly in $C_6D_5NO_2$ was found to be 120 °C with $\Delta G^{\dagger}_{393K}$ = 20.2 kcal mol^{-1}. Although these types of measurements are not very precise (errors are likely to be ±0.5 kcal mol^{-1}),[25,26] clearly the rotational barrier is of somewhat *lower* energy for the incarcerated $(CH_3)_2NCHO$ than for the simply dissolved amide.

When **1**·$(CH_3)_2NCOCH_3$ was submitted to the same experiment, a coalescence temperature of 190 °C was estimated that provided $\Delta G^{\dagger}_{463K}$ = 20.3 kcal mol^{-1} for incarcerated amide rotation around its C–N bond. For $(CH_3)_2NCOCH_3$ simply dissolved in $C_6D_5NO_2$, the coalescence temperature was 63 °C and $\Delta G^{\dagger}_{336K}$ = 18 kcal mol^{-1}. Thus, incarceration of $(CH_3)_2NCOCH_3$ *raises* the barrier to rotation relative to simple dissolution.

The rotational barrier to amide bonds has been studied in many solvents,[26] in the gas phase,[27] and in a polystyrene matrix.[28] Although much ambiguity and controversy remains in interpreting the stereoelectronic factors that control the barrier size,[29] it is clear that the barrier *decreases* in the order polar solvents > nonpolar solvents > gas phase.

If we fit the current results into this correlation, for $(CH_3)_2NCHO$ the barrier *decreases* in the order polar solvent > carcerand inner phase > vacuum. For $(CH_3)_2NCOCH_3$, the barrier *decreases* in the order carcerand inner phase > polar solvent > vacuum. The simplest and most satisfying way of interpreting these orders is as follows. Molecular model examination of **1**·$(CH_3)_2NCHO$ suggests that the carcerand inner phase is a mixture of vacuum and guest volume occupation that leaves the rotating molecular parts of the amide less encumbered by the sides of its container than by solvent molecules in an ordinary solvent medium. In contrast, CPK models of **1**·$(CH_3)_2NCOCH_3$ can barely be assembled because the container sides are compressed against the guest parts. Rotation of the $(CH_3)_2N$ plane out of the $COCH_3$ plane to produce a 90° dihedral angle for the two planes (a transition-state model) appears to require more deformation of the container than the simple planar guest. The rigid container resists deformation more than solvent molecules resist being moved to accommodate the 90° dihedral angle. Thus, the inner phase of carcerands can be designed to be vacuumlike, liquidlike, or even solidlike, depending on the mix of space occupation by guest and of free space.

Effect of Solvent on ^{1}H NMR Spectra of Incarcerated Guest. One of the questions addressed in this investigation is whether solvent molecules in which carceplexes are dissolved or surfaces on which they are absorbed can be affected by the properties of incarcerated guest molecules. A possible way of answering the first question was to see if incarcerated guests were subject to the phenomenon of aromatic solvent-induced shift (ASIS) of proton resonances of solutes with respect to their shifts in nonaromatic solvents.[21,30] The ^{1}H NMR spectrum of $(CH_3)_2NCOCH_3$ in $C_6D_5NO_2$ was compared to that of the same amide in $CDCl_3$. The ^{1}H NMR spectrum of the guest amide of **1**·$(CH_3)_2NCOCH_3$ was then taken in the two solvents. The chemical shift of CH_3COCH_3 served as an external reference in these experiments. Table III records the results for each of the three kinds of protons of $(CH_3)_2NCOCH_3$. Sample dissolution of $(CH_3)_2NCOCH_3$ in the two solvents revealed, as expected, a modest ASIS *upfield* shift for each of the three kinds of guest protons, which averaged δ 0.07 ± 0.03. Dissolution of **1**·$(CH_3)_2NCOCH_3$ in the two solvents resulted in a larger ASIS *downfield* shift for each of the three kinds of protons, which averaged δ 0.30 ± 0.06. The incarcerated $(CH_3)_2NCOCH_3$ proved to be more sensitive to the magnetic properties of the aromatic solvent than simply dissolved $(CH_3)_2NCOCH_3$. Table IV tabulates these results.

A possible explanation is as follows. The shell of the carcerand is composed largely of eight benzenes, each substituted by three adjacent oxygens in the shell's equatorial region and by two alkyl groups and a hydrogen in the arctic region. Thus, the equatorial region of the shell is rich in electronegative atoms, and the arctic region is rich in relatively electropositive C and H atoms. The guest cannot interchange its northern and southern ends, and therefore its parts are subject to the polar gradients of the host mentioned previously. The nitrobenzene as solvent aligns itself on the surface of the carceplex to compensate its dipole to that of the shell by a π–π interaction, an effect transmitted to the π-system of the amide. Thus, the solvent "communicates" with the guest through induced-dipolar effects in the shell's π-system. Directly induced dipolar effects between amide dissolved in nitrobenzene are expected to be more randomized due to movements of solvent and solute with respect to one another, which are rapid on the ^{1}H NMR time scale. Thus, the carcerand provides a more organized interaction between amide and solvent leading to a larger ASIS effect, which is reversed in direction by the shell's dipolar mediation effects.

Table IV. Effect of Incarceration of $(CH_3)_2NCOCH_3$ on the $C_6D_5NO_2$ Solvent-Induced Chemical Shift of the Three Kinds of Protons in the ^{1}H NMR Spectra with $CDCl_3$ as the Standard Solvent and CH_3COCH_3 as an External Reference

	δ of free amide			δ of incarcerated amide		
proton[a]	$CDCl_3$	$C_6D_5NO_2$	$\Delta\delta$	$CDCl_3$	$C_6D_5NO_2$	$\Delta\delta$
l	3.02	2.92	−0.10	+1.04	+1.28	+0.24
m	2.94	2.90	−0.04	−1.46	−1.12	+0.34
n	2.09	2.03	−0.06	−2.40	−2.07	+0.33

[a] See the following structure:

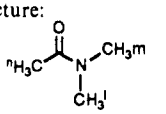

Differences in Chromatographic Properties of Carceplexes. Another form of communication between the guest of a carceplex and external phases is evident in the fact that **1**·$(CH_3)_2NCOCH_3$ has an R_f value of 0.5, while both **1**·$(CH_3)_2NCHO$ and **1**·$(CH_3)_2SO$ have an R_f value of 0.6 on 0.5-mm silica gel plates with 3:1 chloroform–hexanes as the mobile phase. Indeed, when shell closures to form carceplexes were carried out in the $(CH_3)_2NCOCH_3$–$(CH_3)_2NCHO$ mixtures, the two carceplexes formed were easily separated by chromatography. We interpret the effect of guest on the adsorption properties of their carceplexes to guest-induced dipole–dipole interactions between the shell and the silica gel surface. The fact that the directions of the dipoles are more averaged by rapid movement with respect to their shell of $(CH_3)_2SO$ and $(CH_3)_2NCHO$ than with $(CH_3)_2NCOCH_3$ as guest accounts for the observed differences in chromatographic behavior. These experiments suggest that the three carceplexes have dipole moments due to their guests and that their magnitudes change with changes of their guests.

Ultraviolet Spectra. The ultraviolet spectrum of **1**·$(CH_3)_2NCOCH_3$ was very similar to that of cavitand **5**. No charge-transfer bands were observed.

Differences in Infrared Spectra due to Incarceration. The infrared spectrum of **1**·$(CH_3)_2NCHO$ (KBr pellet) provides a single band for $(CH_3)_2NCHO$ (carbonyl stretch) at 1700 cm^{-1}, whereas that of **1**·$(CH_3)_2NCOCH_3$ (KBr pellet) gives *two bands of equal intensity* for $(CH_3)_2NCOCH_3$ (carbonyl stretch) at 1648 and 1665 cm^{-1}. The normal carbonyl band for $(CH_3)_2NCHO$ is 1675 cm^{-1} in its liquid and 1715 cm^{-1} in its gas phase.[31] The normal carbonyl band for $(CH_3)_2NCOCH_3$ is 1640 cm^{-1} in its liquid[32] and 1695 cm^{-1} in its gas phase.[32] Thus, for both amides the incarcerated carbonyl stretch observed in the inner phase of the carceplexes is in between that of the liquid and that of the gas phases. This observation is in harmony with our characterization of the inner phase as being a mixture of empty space, guest, and confining walls, in a sense mixing the gas and liquid phases in a container, but in different proportions depending on the relative amounts

(26) Drakenberg, T.; Dahlqvist, K.-I.; Forsen, S. *J. Phys. Chem.* **1972**, *76*, 2178–2183; Ross, B. D.; True, N. S.; Matson, G. B. *J. Phys. Chem.* **1984**, *88*, 2675–2678.
(27) Feigel, M. *J. Phys. Chem.* **1983**, *87*, 3054–3058.
(28) Chan, B.; Shukla, J. P.; Walker, S. *J. Mol. Struct.* **1983**, *102*, 165–173.
(29) Gryff-Keller, A.; Terpinski, J.; Zajaczkowska-Terpinska, E. *J. Chem. Res. Synop.* **1984**, 330–331.
(30) Ahmed, M.; Phillips, L. *J. Chem. Soc., Perkin Trans. 2* **1977**, 1656–1661.
(31) Jao, T. C.; Scott, I.; Steele, D. *J. Mol. Spectrom.* **1982**, *92*, 1–17.
(32) *The Sadtler Standard Infrared Grating Spectra*; Sadtler Research Laboratories: Philadelphia, 1974; 33010K.

of space occupation and empty space.

The appearance of two carbonyl bands of equal intensity for **1**·$(CH_3)_2NCOCH_3$ and only one for **1**·$(CH_3)_2NCHO$ is interpreted as follows. The crystal structure of **1**·$(CH_3)_2NCOCH_3$ reveals that the northern hemisphere is rotated about 15° relative to the southern hemisphere. This rotation introduces a helical chiral element into the shell of **1**·$(CH_3)_2NCOCH_3$. We speculate that the hybridization at nitrogen in $(CH_3)_2NCOCH_3$ is not sp^2, but is $sp^{2.1}$ or $sp^{2.2}$, which makes the nitrogen and its three attached carbons into a shallow pyramid. This geometry coupled with the barrier to rotation about the OC–N bond of $(CH_3)_2NCOCH_3$ renders the molecule chiral on the infrared time scale ($\sim 10^{-13}$ s). Combining the chiral elements of the shell and the guest provides two diastereomers, each with its own carbonyl stretching band. In principle, **1**·$(CH_3)_2NCHO$ should also be a mixture of diastereomers, but the smaller amide is free to rotate about all axes relative to its shell, providing many diastereomeric species with little difference in their environments and therefore in their carbonyl stretching frequencies. The rotational constraints of incarcerated $(CH_3)_2NCOCH_3$ relative to its shell result in two dominating but different environments for the carbonyl group and, hence, two carbonyl bands.

Comparisons of Carceplexes, Spheraplexes, Cryptaplexes, Caviplexes, Zeolites, and Clathrates. Carceplexes are composed of host and guest components that cannot separate from one another except by the breaking of covalent bonds. Their existence and stability do not depend on host–guest attractions nor on other than gross size complementarity, but upon physical envelopment of guests during shell closures leading to carceplexes. A wide diversity of guests have been trapped in the inner phases of the two similar kinds of carceplexes reported thus far, I and **1**. The guests include metal cations, halide anions, argon, Freon 112 ($ClCF_2CF_2Cl$),[3] amides,[3,4] nitriles,[4] sulfoxides, alcohols,[4] ethers,[3] and ketones.[4] Under neutral, ambient conditions, the dissociation rate constants are in effect infinite, except for very small guests (e.g., H_2O).[3]

Spheraplexes and cryptaplexes exist only because of strong host–guest attractions of a pole–dipole type. Spherands are hollow hosts that are preorganized for having a stereoelectronically complementary relationship with appropriate guests, whereas cryptands are not hollow and undergo conformational reorganizations during complexation. Both spheraplexes and cryptaplexes exhibit substantial activation free energies for dissociation of highly complementary complexing partners. Caviplexes exist by virtue of weak dipole–dipole attractions between complementary complexing partners. Cavitand hosts are rigid enough not to be able to fill their own cavities by conformational reorganizations. Activation free energies for dissociations of caviplexes are ordinarily very low in solution. Zeolites are insoluble polymeric inorganic solids containing enforced channels into which a variety of complementary guests can *enter and depart* depending chiefly on size complementarity and temperature. The zeolites can be thermally emptied of volatile guests and still maintain their structural integrity. Their study is limited to the solid state. Clathrates are crystalline solids of organic compounds containing interstitial solvent (guest) molecules. Channel clathrates are subject to guest exchange between clathrate solids and liquid or gas phases containing potentially exchangeable guests. Clathrate organization depends on intermolecular lattice forces, and when dissolved that organization disappears.

In a conceptual sense, the previous classes of hosts all have inner phases that more or less modify guest properties. However, carceplex interiors are unique in enough ways to justify our referring to them as a new phase of matter: (1) Complexes are closed molecular cells of definable internal volumes that maintain their structural integrity as solids, dissolved solutes, or even as short-lived gases (witness their being subject to DCl ms). (2) Their guests cannot escape except by covalent bond breaking processes. (3) Carceplexes possess discrete molecular properties such as molecular weights, volumes, molecular formulas, and chromatographic behavior and are subject to crystal structure determinations. (4) Carceplex interiors are definable mixtures of free space and space-occupying guests, the relative amounts of which can be designed. Their guests' movements can be highly constrained or more free than in solution, depending on the mix. (5) The only limitations on the guests that can be incarcerated appear to be those of molecular volume and shape. The guest must possess a molecular volume less than that of the inner phase of the carcerand and must have a shape adaptable to that of the carcerand interior. (6) More than one guest and even more than one kind of guest can occupy the inner phase simultaneously, the only limitation being that of available space. (7) The properties of the guest can grossly modify the properties of the carceplex. (8) The solubility properties of carceplexes are subject to control by pendant-group manipulation. (9) The inner phases of carceplexes are unusual and interesting places where chemical reactions might be carried out. Such studies are in progress.

Conclusions

A short, inexpensive synthesis of three new soluble carceplexes is reported, each formed by making eight $ArO–CH_2$ bonds between the rims of two cavitands in solvents whose molecular shapes and sizes were amenable to incarceration. The high yields (49–61%) for the shell closures coupled with the fact that incarceration was a condition of shell closure indicates these reactions to be templated. Complete elemental analyses and prominent M^+ or $M^+ + H$ mass spectral ions were obtained. A crystal structure is reported for **1**·$(CH_3)_2NCOCH_3$, which shows that the long axes of host and guest are coincident and that the northern hemisphere of the carcerand was rotated about 15° with respect to the southern hemisphere. A combination of ^{13}C and ^1H NMR spectra demonstrated that $(CH_3)_2NCOCH_3$ as guest was constrained to rotating only around its long axis (up to 175 °C), that $(CH_3)_2NCHO$ rotated around all axes even at −37 °C, that $(CH_3)_2SO$ rotated around all axes at temperatures above −2 °C but was constrained below that temperature to rotation only about its long axis, and that the rotations of the northern with respect to the southern hemispheres of **1**·$(CH_3)_2SO$ was constrained at −18 °C. Comparisons of the barriers to rotation about the C–N bond of the two incarcerated amides compared to liquid- and gas-phase amides provided the following decreasing orders of barrier free energies: for $(CH_3)_2NCHO$, polar solvent > carcerand inner phase > vacuum, and for $(CH_3)_2NCOCH_3$, carcerand inner phase > polar solvent > vacuum. Thus, the inner phase is composed of a mix of free space, carcerand walls, and space occupation by guest. The chemical shifts of incarcerated $(CH_3)_2NCOCH_3$ protons in ^1H NMR spectra were more sensitive to solvent changes ($CDCl_3$ vs $C_6D_5NO_2$) than freely dissolved $(CH_3)_2NCOCH_3$. Other evidence of communication between incarcerated guest and the carceplex environment was demonstrated by **1**·$(CH_3)_2NCOCH_3$ and **1**·$(CH_3)_2NCHO$ possessing different chromatographic properties. The carbonyl stretching frequencies of the two incarcerated amides were in between those observed in solution and in the gas phase. Incarcerated $(CH_3)_2NCHO$ gave a single band, whereas $(CH_3)_2NCOCH_3$ gave two bands of equal intensity. The latter observation is interpreted as being due to the amide and its shell each possessing chiral elements revealed by the very short IR time scale as different stretching frequencies of two equally populated diastereomeric states. We conclude that carceplexes are molecular cells whose interiors are a new and unique phase of matter in which different amounts of free space, space occupation, and wall surfaces can be designed, prepared, and studied as solids, solutes, or gas-phase mass spectral entities.

These carceplexes in the solid state contain immobile hosts but mobile guests, not dissimilar to the different parts of liquid crystals. We are examining carceplexes for possible material science applications suggested by this and other analogies.

Experimental Section

General Procedures. Chemicals were reagent grade (Aldrich) unless otherwise noted. THF and Et_2O were distilled under N_2 from sodium benzophenone ketyl. Guest solvents $(CH_3)_2NCHO$, $(CH_3)_2NCOCH_3$, and $(CH_3)_2SO$ were stored over 3-Å molecular sieves (activated at 330 °C for 4 h) for several days and degassed at high vacuum immediately prior to use. The ^1H NMR spectra were run on a Bruker WP-200, AF-200, AM-360, or AM-500 spectrometer. Residual ^1H signals from

deuterated solvents were used as a reference unless $(CH_3)_4Si$ (δ 0.00) was present. Mass spectra were run on a Kratos AEI Model MS-9 fitted with a homemade FAB gun for EI and FAB and a VG Analytical ZAB-SE for FAB. The matrix was 3-$NO_2C_6H_4CH_2OH$. Melting points (uncorrected) were measured on a Thomas-Hoover apparatus for those below 250 °C and on a Mel-Temp apparatus otherwise. Silica gel (E. Merck 63–200 μm for flash and 40–63 μm for preparative) was used for chromatography. Silica gel glass-backed analytical plates (0.2 mm, E. Merck) and C_{18} bonded, end-capped reversed-phase preparative and analytical plates (E. Merck) were used. Infrared spectra were taken with a Perkin-Elmer 580 B infrared spectrometer whose data were reduced with a PE 3600 data station. NOE experiments were performed with Bruker AM 500 and AM 360 spectrometers by use of a standard microprogram. Fully decoupled, selectively decoupled, and INEPT ^{13}C NMR spectra were performed with the Bruker AM 360 spectrometer.

5,11,17,23-Tetrabromo-2,8,14,20-tetrakis(2-phenylethyl)pentacyclo-[19.3.1.1^{3,7}.1^{9,13}.1^{15,19}]octacosa-1(25),3,5,7(28),9,11,13(27),15,17,19-(26),21,23-dodecaen-4,6,10,12,16,18,22,24-octol, Stereoisomer (4). To a stirred mixture of 55.1 g of octol **3**[5] in 300 mL of 2-butanone under argon was added over 5 min 52 g of solid *N*-bromosuccinimide (290 mmol, recrystallized and dried[33]). After the mixture was stirred for 12 h at 25 °C, a thick precipitate developed. The solid was filtered and washed with methanol to remove succinimide and then recrystallized from 1800 mL of a 6:1 CH_3CN–$(CH_3)_2NCHO$ (v/v) solution to give 43.3 g of **4** (58%). This compound gives a well-formed spot on reversed-phase silica gel with 80% acetone–20% water–2% NaBr (w) as the mobile phase: mp 260 °C dec; ^1H NMR (200 MHz, $(CD_3)_2CO$) δ 2.58–2.79 (m, 16 H, CH_2CH_2); 4.52 (m, 4 H, $CHCH_2CH_2$); 7.11–7.18 (m, 20 H, C_6H_5); 7.75 (s, 4 H, H_d, Chart IV); 8.36 (s, 8 H, OH); MS (FAB+, NOBA) *m/e* 1220 (M + H$^+$, 30%); 1115 (M + H$^+$ – $PhCH_2CH_2$, 100%). Anal. Calcd for $C_{60}H_{52}Br_4O_8$: C, 59.04; H, 4.29. Found: C, 58.86; H, 4.20.

7,11,15,28-Tetrabromo-1,21,23,25-tetrakis(2-phenylethyl)-2,20:3,19-dimetheno-1*H*,21*H*,23*H*,25*H*-bis[1,3]dioxocino[5,4-*i*:5′,4′-*i*′]benzo[1,2-*d*:5,4-*d*′]bis[1,3]benzodioxocin, Stereoisomer (5). To a stirred mixture of 600 mL of $(CH_3)_2NCOCH_3$, 30 g of K_2CO_3, and 6 mL of CH_2BrCl (93 mmol) was added over 2 days as a solid 21.0 g (17 mmol) of octol **4**. An additional 5 mL of CH_2BrCl (17 mmol) was added, and the reaction mixture was warmed to 40 °C and stirred for 1 day. An additional 5 mL of CH_2BrCl was added, and the reaction mixture was warmed to 65 °C for 3 days during which the formation of much precipitate was observed. The reaction mixture was cooled, and the solvent was removed in vacuo. The residue was stirred in water and extracted with $CHCl_3$. The $CHCl_3$ solution was concentrated under vacuum and chromatographed on a gravity column of 500 g of silica gel and eluted with 1:1 $CHCl_3$–$(CH_2)_6$ as the mobile phase. The isolated product was recrystallized from $CHCl_3$–CH_3OH and dried at 10^{-5} Torr for 1 day at 160 °C to give 11 g of **5** (52%): mp 280–290 °C dec; ^1H NMR (200 MHz, $CDCl_3$) δ 2.52 (m, 8 H, $CHCH_2CH_2$)*; 2.68 (m, 8 H, $CHCH_2CH_2$)*; 4.42 (d, 4 H, inner of OCH_2O, J = 7.3 Hz); 4.96 (t, 4 H, $CHCH_2CH_2$, J = 8 Hz); 5.98 (d, 4 H, outer of OCH_2O, J = 7.3 Hz); 7.09–7.23 (m, 24 H, C_6H_5, H_d, Chart IV). Those marked by * are based on decoupling of $CHCH_2CH_2$; MS (FAB+, NOBA) *m/e* 1269 (M + H$^+$, 100%). Anal. Calcd for $C_{64}H_{52}Br_4O_8$: C, 60.59; H, 4.13. Found: C, 60.52; H, 4.04.

1,21,23,25-Tetrakis(2-phenylethyl)-2,20:3,19-dimetheno-1*H*,21*H*,23*H*,25*H*-bis[1,3]dioxocino[5,4-*i*:5′,4′-*i*′]benzo[1,2-*d*:5,4-*d*′]bis[1,3]benzodioxocin-7,11,15,28-tetrol, Stereoisomer (2). To a flame-dried flask were added 600 mL of dry THF and 5.0 g of the tetrabromide **5** (3.9 mmol). After the stirring mixture was cooled to −78 °C, 35 mL of 1.7 M *tert*-butyllithium–pentane solution (60 mmol) was added. After 1 min, 12 mL of $B(OMe)_3$ (105 mmol) was added. The reaction mixture was then warmed to ambient temperature and stirred for 1 h. After the mixture was cooled again to −78 °C, 100 mL of a 1.5 M NaOH–15% H_2O_2 solution was added. This mixture was warmed to ambient temperature and stirred for 3 h. Careful addition of 20 g of $Na_2S_2O_5$ followed by removal of the THF in vacuo left a white solid in the residual water that was filtered and washed with water. This sample was dry loaded (by dissolving it in THF, adding silica gel, and removing solvent) onto a silica gel gravity column that was eluted with 3:1 EtOAc–hexanes, which afforded separation of the tetrol **2** from the triol **7**. Each alcohol was recrystallized from THF–methanol and dried at 10^{-5} Torr for 24 h at 130 °C to give 2.1 g of the tetrol **6** (53%) and 900 mg of the triol **7** (23%). For tetrol **2**: mp 300 °C dec; ^1H NMR (200 MHz, $(CD_3)_2CO$) δ 2.58–2.68 (m, 16 H, CH_2CH_2); 4.42 (d, 4 H, inner OCH_2O, J = 7 Hz); 4.78 (t, 4 H, $CHCH_2CH_2$, J = 8 Hz); 5.83 (d, 4 H, outer OCH_2O, J = 7 Hz); 7.14 (s, 4 H, H_d, Chart IV); 7.20 (m, 20 H, C_6H_5); 7.88 (s, 4 H, OH); MS (FAB+, NOBA) *m/e* 1016 (M + H$^+$, 100%). Anal. Calcd for $C_{64}H_{56}O_{12}$: C, 75.58; H, 5.55. Found: C, 75.41; H, 5.51.

1,21,23,25-Tetrakis(2-phenylethyl)-2,20:3,19-dimetheno-1*H*,21*H*,23*H*,25*H*-bis[1,3]dioxocino[5,4-*i*:5′,4′-*i*′]benzo[1,2-*d*:4,5-*d*′]bis-[1,3]benzodioxocin-7,11,15-triol, Stereoisomer (7). This compound was a byproduct in the preparation of **2**: mp 300 dec; ^1H NMR (200 MHz, $(CD_3)_2CO$) δ 2.63 (m, 16 H, CH_2CH_2); 4.44 (dd, 4 H, inner of OCH_2O, J = 7.3 Hz); 4.80 (t, 4 H, $CHCH_2CH_2$, J = 7 Hz); 5.82 (dd, 4 H, outer of OCH_2O, J = 7.3 Hz); 6.56 (s, 1 H, Ar*H*, ortho to O's); 7.16 (s, 3 H, H_d, Chart IV); 7.20 (m, 20 H, C_6H_5); 7.66 (s, 1 H, H_d, Chart IV); 7.95 (s, 1 H, O*H*); 7.97 (s, 2 H, O*H*); MS (FAB+, NOBA) *m/e* 1002 (M + H$^+$, 100%). Anal. Calcd for $C_{64}H_{56}O_{11}$: C, 76.78; H, 5.64. Found: C, 77.09; H, 5.74.

1,15,23,25,47,49,57,67-Octakis(2-phenylethyl)-31,41-(epoxymethanoxy)-17,21:51,55-dimethano-2,46:14,26-dimetheno-3,45,13,27-(methynoxymethanoxymethyno)-1*H*,15*H*,23*H*,25*H*,47*H*,49*H*-bis[1,3]benzodioxocino[9,8-*d*:9′,8′-*d*′]bis[1,3]benzodioxocino[9′,10′:14,15;-10″,9″:19,20][1,3,6,8,11,13,16,18]octaoxacycloeicosino[4,5-*j*:10,9-*j*′]bis-[1,3]benzodioxocin, Stereoisomer Containing Dimethyl Sulfoxide (1·(C-$H_3)_2SO$). To a flame-dried flask were added under argon 400 mL of $(CH_3)_2SO$ (stored over sieves and degassed immediately prior to use) and 1.3 g of Cs_2CO_3 (4.0 mmol). The reaction mixture was warmed with stirring to 60 °C. A solution of 520 mg of tetrol **2** (0.51 mmol) and 100 μL of CH_2BrCl 1.5 mmol) in 40 mL of $(CH_3)_2SO$ (similarly treated) was added with a syringe pump over 10 h. When the addition was complete, the reaction mixture was warmed to 100 °C and an additional 50 μL of CH_2BrCl were added every 10 h for 3 days. The reaction mixture was cooled and the solvent was removed in vacuo. The crude residue was stirred in water and extracted with $CHCl_3$. Silica gel was added to the $CHCl_3$ solution, and the $CHCl_3$ was removed in vacuo. This silica gel adsorbed sample was dry loaded onto a 100-g silica gel column and eluted with 3:1 $CHCl_3$/hexanes to give 335 mg of **1**·$(CH_3)_2SO$ (61%), which was recrystallized from $CHCl_3/CH_3CN$.

Carceplex **1**·$(CH_3)_2NCOCH_3$ was prepared as described previously (54%). Carceplex **1**·$(CH_3)_2NCHO$ was prepared as described previously (49%). Melting points for all three carcerands were >360 °C. Mass spectral and NMR data are reported in the Results and Discussion section. The elemental analyses are as follows. For **1**·$(CH_3)_2SO$, Anal. Calcd for $C_{134}H_{118}O_{25}S$: C, 74.51; H, 5.51; O, 18.51; S, 1.48. Found: C, 74.30; H, 5.45; O, 18.40; S, 1.60. For **1**·$(CH_3)_2NCOCH_3$, Anal. Calcd for $C_{136}H_{121}O_{25}N$: C, 75.30; H, 5.62; O, 18.44; N, 0.65. Found: C, 75.34; H, 5.66; O, 18.30; N, 0.60. For **1**·$(CH_3)_2NCHO$, Anal. Calcd for $C_{135}H_{119}O_{25}N$: C, 75.23; H, 5.57; O, 18.56; N, 0.65. Found: C, 75.21; H, 5.52; O, 18.39; N, 0.61.

Crystal Structures. Compound **5** crystallizes from CH_2Cl_2 as small colorless parallelepipeds in the orthorhombic system *Pmcn* (standard setting *Pnma*). Unit cell dimensions are as follows: a = 20.200 (2) Å, b = 12.011 (1) Å, c = 24.675 (4) Å, V = 6004 Å^3, Z = 4 (eight half-molecules related by a mirror plane at x = 1/4). The crystal was examined on a modified Picker FACS-1 diffractometer, Mo Kα radiation, at 295 K. The structure was determined by heavy-atom methods. Refinement of 164 parameters (1699 reflections with $I > 3\sigma(I)$) has an agreement value, R, currently at 0.074. Water seems to be present in interstitial positions with occupancy 0.5.

Compound **1**·$(CH_3)_2NCOCH_3$·5$CHCl_3$ crystallizes from $CHCl_3$ as colorless platelets in the triclinic system *P*$\bar{1}$. Unit cell dimensions are as follows: a = 16.302 (3) Å, b = 18.940 (3) Å, c = 23.182 (4) Å, α = 90.223 (6)°, β = 93.970 (7)°, γ = 102.383 (7)°, V = 6973 Å^3, Z = 2. The crystal was sealed in a capillary with solvent and was examined on a modified Syntex P$\bar{1}$ diffractometer, Cu Kα radiation, at 295 K. The structure was determined by direct methods. Refinement of 3 blocks of 345, 185, and 149 parameters (6126 reflections with $I > 3\sigma(I)$) has an agreement value, R, currently at 0.184. The crystal contains additional uncharacterized, probably disordered solvent molecules.

Further crystallographic details will be published elsewhere.

(33) Perrin, D. D.; Armarego, W. L. F.; Perrin, D. R. *Purification of Laboratory Chemicals*, 2nd ed.; Pergamon Press: Oxford, 1980; p 141.